NUMERICAL SIMULATION VALIDATION AND RESEARCH ON SHIELD CHARACTERISTICS OF BASALT FIBER WOVEN AND AL-MESH BUMPER

B. Jia[(1)], X. Fu[(2)], Y. Wang[(3)], B. J. Pang[(1)]

[(1)] Hypervelocity Impact Research Centre, P O Box 3020, Science Park, Harbin Institute of Technology, ZIP: 150080, China, Email: jiabin@hit.edu.cn
[(2)] J.C.Wu Center for Aerodynamics, Shanghai Jiao Tong University, Shanghai 200240, China, Email: air050352@163.com
[(3)] AVIC China Helicopter Research and Development Institute, Jiangxi 333001, China, Email: wangyangcumt886@126.com

ABSTRACT

Basalt fiber woven as a new type of shielding material has many favorable characteristics while subjected to hypervelocity impact of space debris. A geometrical model for numerical simulation was setup based on the real structure of basalt fiber woven and Al-mesh, and the simulation method is validated through comparison with experiment results. Four types of bumper combination of basalt fiber woven and Al-mesh were presented and the influence of different bumper positions on consumption of kinetic energy of projectile was investigated through numerical simulation. The difference of capability to fragment projectile was also analyzed between basalt fiber woven and Al-mesh.

1 INTRODUCTION

The world space industry continue to rapid development since entering the 21st century, but its byproduct-"space debris" problem has become more serious, which threats on-orbit spacecraft and astronaut [1]. In 1947，Whipple found that setting a protective bumper in front of the rear wall could significantly decrease the probability of a catastrophic failure [2]. Based on this idea, several advanced structures have been invented.

In spite of these advances, attempts continue to be made to find a structure and material for the bumper that will provide better fragmentation of the projectile. For instance, Stuffed Whipple Shield which contains an intermediate blanket of ceramic cloth and high-strength cloth between the Whipple bumper and rear wall is particularly effective if shield standoffs are short [3], and the experimental result of Multi-Shock Shield which sets four or five bumpers in front of the rear wall indicates it is lighter in terms of areal density by up to 33%, but is as effective as the heavier single Whipple Bumper Shield under similar impact conditions at about 10 km/s [4], and Mesh Double-bumper Shield was developed to demonstrate that a Whipple shield could be “augmented” or modified to substantially improve protection by adding a mesh a short distance in front of the Whipple bumper and inserting a layer of high strength fabric between the second bumper and rear wall [5]. As for materials, high strength fiber materials such as Kevlar and Nextel have been used in these structures. In addition, a new type of material-basalt fiber woven has being tested because of its high specific strength, high specific modulus and other favorable characteristics. It is reported that basalt fiber woven/aluminum Stuffed Whipple Shield has better protection performance than the single Whipple Bumper Shield and Nextel/Kevlar Stuffed Whipple Shield with the same areal density of the bumpers at the velocity region from 3.5km/s to 4.8km/s, and the erosion damage of the front surface of the projectile could be observed from the flash x-rays shadowgraphs of the projectiles [6].

Numerical simulation is a good method to obtain detailed shield characteristics of such materials. To simulate the hypervelocity impact on basalt fiber woven bumper, a three-dimensional geometrical model was setup based on the real structure of basalt fiber woven and the material model was chosen appropriately using ANSYS LS-DYNA. The simulation was validated through comparison with results of hypervelocity impact experiment.

Contrary to these new materials, Al-mesh is a traditional protective material which has an outstanding capability when disrupting a projectile. As a result, a special shield using basalt fiber woven in company with Al-mesh could achieve excellent performances. Four types of bumper combination of basalt fiber woven and Al-mesh were presented and the influence of different bumper positions was investigated through numerical simulation of hypervelocity impact by Al-sphere projectile. The shield characteristics of different bumper types were compared with each other by means of numerical simulation and a three-dimensional geometrical model was also setup based on the real structure of Al-mesh. Furthermore, the difference of capability of fragmentation of projectile was analyzed between basalt fiber woven and Al-mesh.

Proc. ‘6th European Conference on Space Debris’
Darmstadt, Germany, 22–25 April 2013 (ESA SP-723, August 2013)

2 NUMERICAL SIMULATION METHOD

2.1 Geometrical model of basalt fiber woven

The basalt fiber woven used has a special structure of fiber weave, as shown in Fig. 1. The single fiber has a diameter as small as 7μm, and a square fiber woven with 20cm side length can contain fibers as many as hundreds of thousand. As a result, the computer memory will be seriously inadequate if a real geometrical model of basalt fiber woven was set up. The model must be simplified to save memory and reduce computing time. The smallest model element was chosen to be the warp yarn and the weft yarn, as shown in Fig. 2.

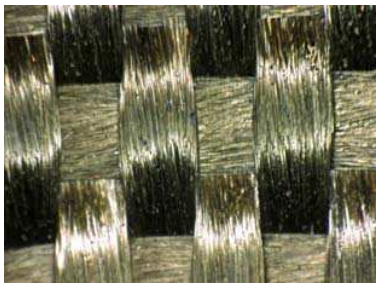

Figure 1. Real structure of basalt fiber woven

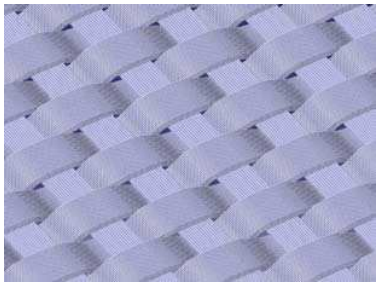

Figure 2. Geometrical model of basalt fiber woven

2.2 Material model of basalt fiber woven

The basalt fiber woven is a kind of quasi-orthotropic inhomogeneous material with discontinuity characteristic, and the strain rate has a major influence on its dynamic behaviour. As strain rate increases, the elastic modulus of basalt fiber increases while failure strain decreases, and the material behaviour intends to be brittle. The tensile modulus, the maximum tensile stress and the failure strain has a variation rule respectively in accordance to strain rate as follows [7]. And the dynamic stress-strain curves of basalt fiber woven under different strain-rate loadings are shown in Fig. 3 [7].

$$E = 105.44 - 4374\exp\left(-\frac{\dot{\varepsilon}}{2283.10}\right) \quad (1)$$

$$\sigma_{\max} = 2956.59 - 1385.08\exp\left(-\frac{\dot{\varepsilon}}{8419.09}\right) \quad (2)$$

$$\varepsilon_{\max} = 2.42 - 0.67\exp\left(-\frac{\dot{\varepsilon}}{1025.19}\right) + 0.16\exp\left(-\frac{\dot{\varepsilon}}{37.89}\right) \quad (3)$$

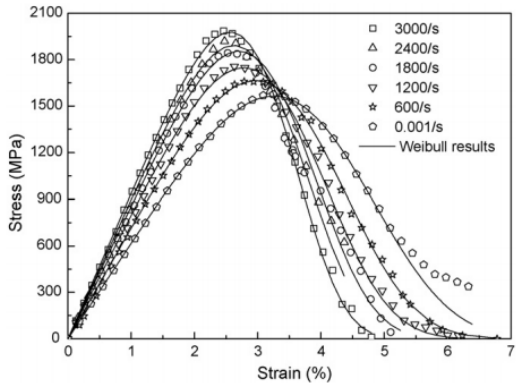

Figure 3. Dynamic stress-strain curves of basalt fiber woven under different strain-rate loadings

The material model of basalt fiber was selected to be the PLASTIC_KINEMATIC model provided in [8] and [9], which neglects the influence of temperature rise on mechanical behaviour of the material.

2.3 Validation of the simulation method

Hypervelocity impact experiment on single basalt fiber woven bumper was conducted in order to validate the numerical simulation method presented. The shield configuration is shown in Fig. 4. The observation plate was a 5A06 Al plate with 1mm in thickness, and the distance between the basalt fiber woven and the observation plate was 50mm. The projectile was a 2017 Al sphere with 3.97mm in diameter and the impact velocity was 3.08 km/s normal to the surface.

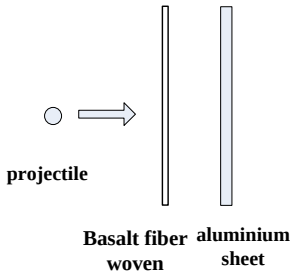

Figure 4. Schematic figure of the shield tested

ANSYS LS-DYNA was adopted and the 3D SPH solver was used to simulate the case tested. The smooth length was set to be 1.05mm in the solver. The comparison of target damage between experiment and simulation are

shown in Fig. 5.

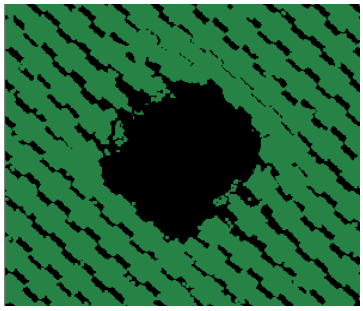

a. Damage of basalt fiber woven by simulation

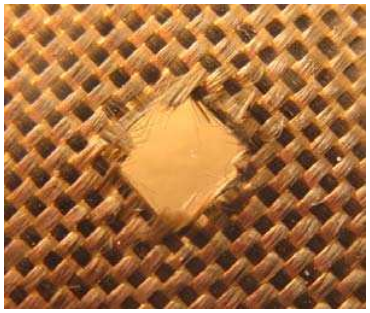

b. Damage of basalt fiber woven by experiment

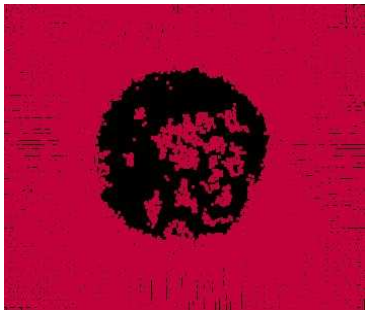

c. Damage of Al plate by simulation

d. Damage of Al plate by experiment

Figure 5. Comparison of target damage between experiment and simulation

The shape of the hole in basalt fiber woven obtained by simulation is essentially the same as that of experiment. The hole is basically a square but the four corners are smooth. The comparison of the fiber woven hole sizes between simulation and experiment is shown in Tab. 1.

Table 1. Hole sizes of basalt fiber woven by simulation and experiment

	Max size along weft yarn(mm)	*Max size along warp yarn(mm)*
Simulation	*4.25*	*4.10*
Experiment	*4.18*	*4.20*
Relative error	*1.65%*	*2.44%*

The damage of the Al observation plate is mainly a round hole for the both. The diameter of the hole is 6.87mm by simulation and 6.86mm by experiment. The relative error is 0.16%.

It can be seen from the data comparison between simulation and experiment that the error of numerical simulation is within acceptable range, and the simulation method presented is validated.

3 SHIELD CHARACTERISTICS OF THE COMBINED BUMPER

3.1 Bumper configurations

Four types of bumper combination of basalt fiber woven and Al-mesh were presented and the influence of different bumper positions was investigated through numerical simulation of hypervelocity impact by Al-sphere projectile.

The basalt fiber woven used had an areal density of 0.022g/cm^2 and two layers were used together without any spacing in between. The mesh count of the Al-mesh was 28*28 and the mesh had an areal density of 0.0325g/cm^2, also two layers used together with no spacing. The total shield space was 40mm for all four shields and the observation plate was an Al 5A06 plate of 0.5mm in thickness for each.

The first type of bumper was basalt fiber woven in front and Al-mesh in behind, and they were closely tied to each other without any spacing in between, which we called in short preposition-no-spacing of basalt fiber woven. The second type of bumper was formed by exchanged in position of the two materials in the first bumper, named as postposition-no-spacing. The third type of bumper was basalt fiber woven in front and Al-mesh in behind but positioned at the middle of the total shield space, called preposition-equal-spacing. And the fourth bumper was formed by exchanged in position of the two materials in the third bumper, named as postposition-equal-spacing. The four types of bumpers are shown in Fig. 6.

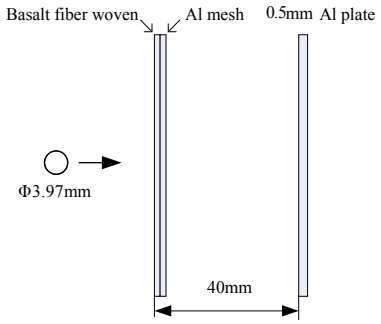

a. preposition-no-spacing

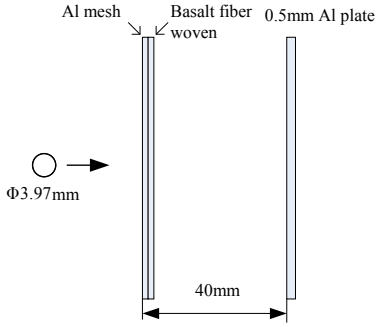

b. postposition-no-spacing

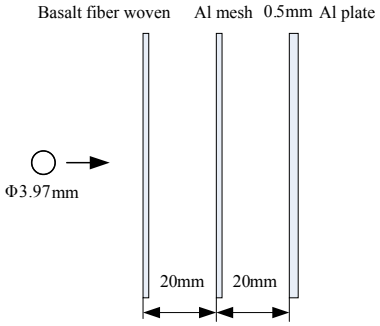

c. preposition-equal-spacing

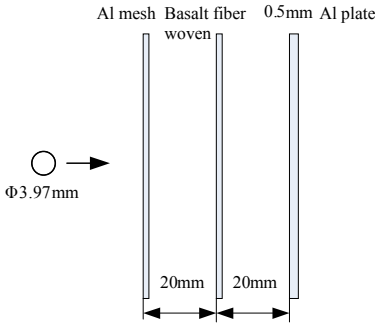

d. postposition-equal-spacing

Figure 6. four types of bumpers with different positions of basalt fiber woven

3.2 Influence of basalt fiber woven position on kinetic energy of projectile

The projectile was 2017 aluminum sphere with the diameter of 3.97mm, and the impact angle was 0 degree. The projectile velocity was set to be 5km/s and the influence of different bumper positions on consumption of kinetic energy of projectile was investigated through numerical simulation. Further more, a three-dimensional geometrical model was also setup based on the real structure of Al-mesh, as shown in Fig. 7 and 8.

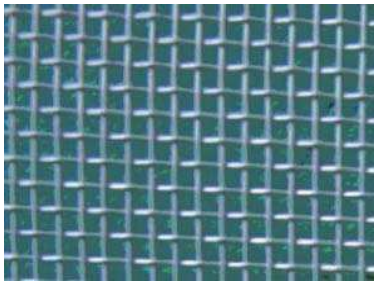

Figure 7. Real structure of Al-mesh

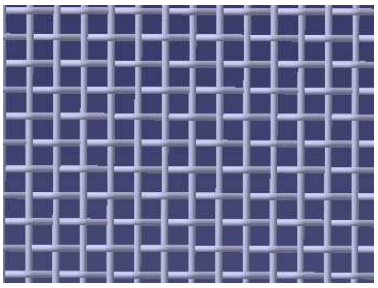

Figure 8. Geometrical model of Al-mesh

The relationship curves of kinetic energy of projectile vs time for the 4 shields are shown in Fig. 9. It can be seen that the ability to consume kinetic energy of projectile is sorted in descending sequence to be postposition-equal-spacing, preposition-equal-spacing, postposition-no-spacing and preposition-no-spacing. This can be interpreted as that at 5km/s, the ability of bumper to consume kinetic energy of projectile can be elevated effectively if basalt fiber woven is put behind Al mesh at certain distance.

The Al-mesh absorbs kinetic energy of projectile differently if the mesh position is changed in the 4 shields. The relationship curves of kinetic energy of the second Al-mesh vs time for the 4 shields are shown in Fig. 10. It can be seen that the kinetic energy of the mesh achieves a peak value after the full penetration of projectile. The peak value of preposition-equal-spacing is the highest, but the energy of mesh descends afterwards for the 4 shields in a certain degree. This is because the secondary debris of this Al-mesh, produced by impact of projectile, will impact the shield layer behind and transfer part of their kinetic energy to the

shield layer behind or transform into heat energy. In the case of preposition of basalt fiber woven, the secondary debris of Al-mesh will impact directly the observation plate behind, and the degree of descending of its kinetic energy is much higher than that of postposition of fiber woven. In particular case of preposition-equal-spacing, more than half of peak kinetic energy of Al-mesh is finally absorbed by observation plate. As a result, the impact energy on observation plate in preposition-equal-spacing comes from the secondary debris of Al-mesh to a large extent.

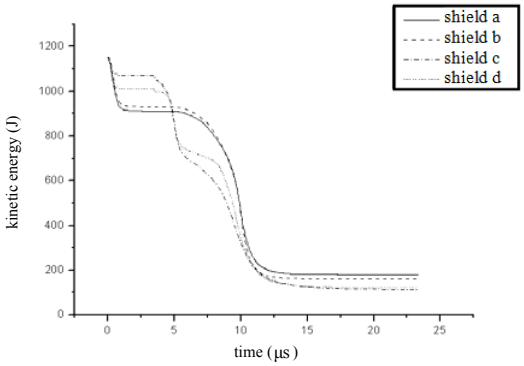

Figure 9. Relationship curves of kinetic energy of projectile vs time for the 4 shields

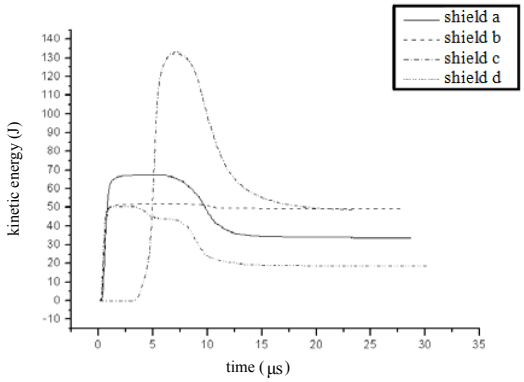

Figure 10. Relationship curves of kinetic energy of the second Al-mesh vs time for the 4 shields

3.3 Different ability to fragment projectile for basalt fiber woven and Al-mesh

In the case of preposition-equal-spacing, after projectile penetration of basalt fiber woven, the front part of projectile mainly undertakes compression deformation due to the high strength and high elastic modulus of basalt fiber woven. Severe fragmentation of projectile does not show up and the back part of projectile basically keeps intact. The projectile does not fragment totally until full penetration of Al-mesh behind, as shown in Fig. 11.

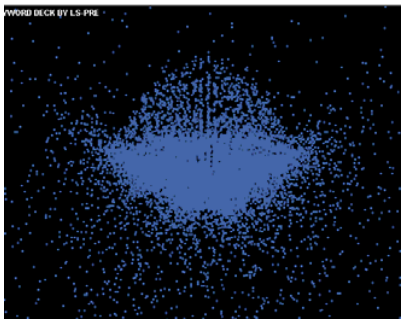

a. projectile after penetration of basalt fiber woven

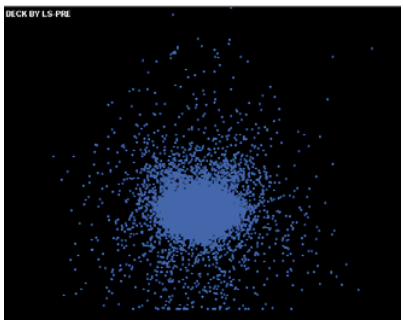

b. projectile after penetration of Al-mesh

Figure 11. Fragmentation shape of projectile in preposition-equal-spacing

If the stress state of projectile is analyzed during its penetration process of basalt fiber woven and Al-mesh, we can find that Al-mesh has obvious more cutting effect on projectile as a whole than that of basalt fiber woven. Meanwhile, basalt fiber woven has better shield capability against smaller debris and expansion of debris cloud than that of Al-mesh. One of the reasons is that the special grid structure of Al-mesh has a energy concentration effect on impacting projectile whose diameter is bigger than that of Al-wire in mesh, which is equivalent to Al-wire cutting projectile directly in high speed. The other reason is that some of small fragments can go through the grid hole of Al-mesh directly without subjecting to any impedance from Al-mesh. Although basalt fiber woven also has an energy concentration effect, its fibers are too thin to show up obvious energy concentration effect for projectile with large diameter. Thus the projectile as a whole is stressed in a comparatively even way. As a result, shield configuration with basalt fiber woven behind Al-mesh can exploit the shield advantages of the two materials both to the full. The stress state of front part of projectile is shown in Fig. 12 when impacting basalt fiber woven and Al-mesh respectively.

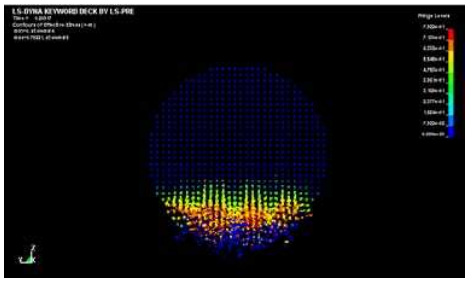

a. projectile impacting basalt fiber woven

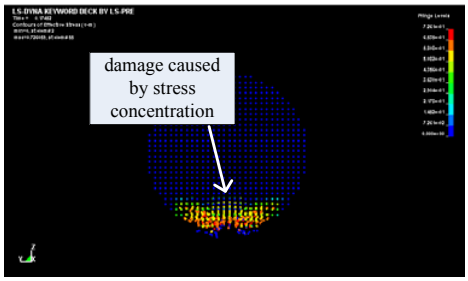

b. projectile impacting Al-mesh

Figure 12. Stress profile of projectile when impacting basalt fiber woven or Al-mesh

4 CONCLUSIONS

A geometrical model for numerical simulation was setup based on the real structure of basalt fiber woven and Al-mesh. And the material model of basalt fiber was appropriately selected. The numerical simulation method is validated through comparison of simulation results with hypervelocity impact experiment results. Four types of bumper combination of basalt fiber woven and Al-mesh were presented and the influence of different bumper positions on consumption of kinetic energy of Al-sphere projectile hypervelocity impact at normal incidence was investigated through numerical simulation. The results indicated that the ability of bumper to consume kinetic energy of projectile can be elevated effectively if basalt fiber woven is put behind Al mesh at certain distance. Analyses of stress state of projectile during its penetration process of basalt fiber woven and Al-mesh showed that Al-mesh has obvious more cutting effect on projectile as a whole than that of basalt fiber woven. Meanwhile, basalt fiber woven has better shield capability against smaller debris and expansion of debris cloud than that of Al-mesh.

ACKNOWLEDGEMENTS

This work was supported by Project of Space Debris Research of China National Defence Science and Industry Bureau (KJSP09205) and Project of Key Laboratory Opening Funding of Technology of Micro-Spacecraft (HIT.KLOF.2011.01507376).

REFERENCES

1. Christiansen, E.L. (2003). *Meteoroid/Debris Shielding*, NASA TP-2003-210788.
2. Whipple, F.L. (1947). Meteorites and space travel. *Astronomical Journal*, **52**, 132-137.
3. Christiansen, E.L. (1995). Enhanced meteoroid and orbital debris shielding. *International Journal of Impact Engineering*, **17**, 217-228.
4. Boslough, M.B., Ang, J.A. & Chhabildas, L.C. (1993). Hypervelocity testing of advanced shielding concepts for spacecraft against impacts to 10 km/s. *International Journal of Impact Engineering*, **14**, 95-106.
5. Christiansen, E.L. & Kerr, J.H. (1993). Mesh double-bumper shield: A low-weight alternative for spacecraft meteoroid and orbital debris protection. *International Journal of Impact Engineering*, **14**, 169-180.
6. Ha, Y., Pang, B.J., Guan, G.S. & Zhang, W. (2007). Damage of high velocity impact on basalt-glass fiber hybrid woven Whipple Shield. In *Proceedings of the 58th International Astronautical Congress*, 1902~1906.
7. Zhu, L.T., Sun, B.Z., Hu, H. & Gu, B.H. (2010). Constitutive equations of basalt filament tows under quasi-static and high strain rate tension. *Materials Science and Engineering: A*. **527**(13-14), 3245-3252.
8. Barauskas, R. (2005). Combining mezzo- and macro-mechanical approaches in a computational model of a ballistic impact upon textile targets. In *Proceedings of the 5th WSEAS International Conference on Simulation, Modeling and Optimization*, 427-432.
9. Barauskas, R. & Abaraitiene, A. (2007). Computational analysis of impact of a bullet against the multilayer fabrics in LS-DYNA. *International Journal of Impact Engineering*. **34**, 1286-1305.